



# Inhibition of hepatitis C virus by *Avicennia marina* (Forssk.) Vierh. leaves extract: Liquid chromatography-high-resolution mass spectrometry, network pharmacology, molecular simulation, and *in vitro* study

Muhammad Arba<sup>1\*</sup>, Sunandar Ihsan<sup>1</sup>, Fathar Muhamad Irfansya Hatma<sup>1</sup>, Jamili Jamili<sup>2</sup>, Setyanto Tri Wahyudi<sup>3</sup>, Tutik Sri Wahyuni<sup>4</sup>

<sup>1</sup>Department of Pharmaceutical Analysis and Medicinal Chemistry, Faculty of Pharmacy, Universitas Halu Oleo, Kendari, Indonesia

<sup>2</sup>Department of Biology, Faculty of Science, Universitas Halu Oleo, Kendari, Indonesia

<sup>3</sup>Department of Physics, IPB University, Bogor, Indonesia

<sup>4</sup>Department of Pharmaceutical Science, Faculty of Pharmacy, Universitas Airlangga, Indonesia

## ARTICLE INFO

**Article Type:**  
Original Article

**Article History:**  
Received: 7 Jan. 2025  
Revised: 28 Feb. 2025  
Accepted: 4 Mar. 2025  
published: 1 Apr. 2025

**Keywords:**  
Mangrove  
Antiviral activity  
Molecular docking  
Molecular dynamics  
Interleukin

## ABSTRACT

**Introduction:** *Avicennia marina* (Forssk.) Vierh. is known for its antiviral property. However, therapeutic mechanisms of the plant against hepatitis C virus (HCV) are still unclear. Therefore, this study aimed to determine the potential of *A. marina* leaves extract to inhibit HCV infection. The study procedures were carried out using a network pharmacology approach based on liquid chromatography-high-resolution mass spectrometry (LC-HRMS) data.

**Methods:** LC-HRMS was performed to identify the chemical composition of *A. marina* methanolic extract, while network pharmacology was carried out to determine protein targets and signaling pathways in HCV associated with *A. marina*. In addition, molecular docking and dynamic simulations were used to understand molecular interaction of each single compound with its single protein target, followed by *in vitro* testing to validate the computational results.

**Results:** The results of LC-HRMS analysis identified the presence of 74 compounds in the extract, with 70 adhering to Lipinski's Rule of Five. Network pharmacology analysis showed 88 potential therapeutic targets. Molecular docking performed on the top 3 protein targets (Interleukin-6/IL-6, signal transducer and activator of transcription 3/STAT3, and tumor necrosis factor- $\alpha$ /TNF- $\alpha$ ) showed that 2 compounds, Comp28 and Comp63, had the potential to inhibit IL-6, while 3 compounds, Comp4, Comp7, and Comp48, were identified as potential inhibitors of TNF- $\alpha$ . *In vitro* test against HCV demonstrated an IC<sub>50</sub> value of 12.664  $\pm$  0.984  $\mu$ g/mL.

**Conclusion:** This study suggests that *A. marina* leaves extract can act on IL-6, STAT3, and TNF for inhibiting HCV.

### Implication for health policy/practice/research/medical education:

The results of this study provide scientific evidence for understanding molecular mechanisms of *A. marina* to treat HCV infection.

**Please cite this paper as:** Arba M, Ihsan S, Hatma FMI, Jamili J, Wahyudi ST, Wahyuni TS. Inhibition of hepatitis C virus by *Avicennia marina* (Forssk.) Vierh. leaves extract: Liquid chromatography-high-resolution mass spectrometry, network pharmacology, molecular simulation, and *in vitro* study. J Herbmed Pharmacol. 2025;14(2):188-199. doi: 10.34172/jhp.2025.52905.

## Introduction

Hepatitis C virus (HCV) is a significant public health concern, with a global prevalence of 0.5% to 4% and a high risk of progression to chronicity (1). The virus is primarily

transmitted through blood, and high-risk groups include recipients of unscreened blood transfusions, intravenous drug abusers, and hemophiliacs (2). Several studies have shown that chronic HCV infection can lead to severe liver

\*Corresponding author: Muhammad Arba,  
Email: muh.arba@uho.ac.id

damage, including cirrhosis and hepatocellular carcinoma (3,4). To overcome the condition, treatment options, such as interferon therapy and combination therapy with interferon  $\alpha$ -2b and ribavirin have shown some efficacy but relapse rates remain high (4).

Current HCV therapies, including direct-acting antivirals and host-targeting agents have significantly improved treatment outcomes achieving cure rates exceeding 90% (5). However, their high cost and limited access remain major concerns during the treatment process (6). To address these issues, there is a need for affordable solutions and strategies to discover alternative HCV antivirals. Natural resources, such as medicinal plant extracts have shown high potential for developing anti-HCV agents (7), offering more affordable and accessible treatment options.

Mangrove plants are commonly used in traditional medicine due to the presence of abundant secondary metabolites. Different parts of the plants possess specific curative and protective properties against various diseases, including leprosy, ulcers, tuberculosis, elephantiasis, and malaria (8). Parthiban et al reported compounds isolated from mangrove exhibiting various biological activities, such as antioxidant, hepatoprotective, antimicrobial, antidiarrheal, antifeedant, insecticidal, and cytotoxic properties (8). In addition, the plants have been reported to yield a variety of biologically active compounds, including flavonoids, terpenoids, tannins, saponins, steroids, alkaloids, glycosides, and carotenoids (8,9).

*Avicennia marina* is a mangrove species known for its diverse bioactive compounds, including flavonoids, tannins, steroids, saponins, alkaloids, glucosides, and triterpenoids. Leaves, stems, and roots have been reported to be rich in alkaloids, terpenoids, and flavonoids (10). In addition *A. marina* has exhibited multiple pharmacological properties, such as anti-cancer, antioxidant, antibacterial, antifungal, antiviral, and anti-inflammatory effects (7). Zandi et al demonstrated the efficacy of *A. marina* extract against herpes simplex virus type 1 (HSV-1) and poliovirus *in vitro* (11). Betulinic acid extracted from the plant also showed antiviral activity against HCV by suppressing COX-2 expression (12). Sheela Devi et al reported that its leaves had an antibacterial effect against bacteria responsible for urinary tract infection (13). Alshehri and Alshehri used the network pharmacology method to identify the potential compounds of *A. marina* retrieved from literature review in the treatment of breast cancer (14).

Despite the existing literature, detailed mechanistic studies explaining how phytoconstituents from *A. marina* interact with HCV proteins at the molecular level are limited. This is the first report on *A. marina* potential in treating HCV infection using network pharmacology method based on liquid chromatography-high-resolution mass spectrometry (LC-HRMS) data. In this current study,

the chemical composition of *A. marina* methanolic extract was identified using LC-HRMS analysis, which allowed known and unknown bioactive compounds profiling of the plant. Network pharmacology study based on LC-HRMS data was then carried out for further analysis. This method is often used to evaluate the therapeutic potential of herbal plants due to their complex matrices nature in multi-component and multi-target pathway paradigm (15). By constructing component-target networks or enriching pathways in Kyoto Encyclopedia of Genes and Genomes (KEGG), protein targets and signaling pathways associated with *A. marina* and HCV were identified. Molecular docking method was applied to understand the interaction of each compound with its single protein target, which offered deeper insights into their protein-ligand interactions. In addition, *in vitro* test of *A. marina* leaves extract against HCV was performed.

## Materials and Methods

### Plant material and extraction process, LC-HRMS analysis, and drug-likeness prediction

*Avicennia marina* (Forssk.) Vierh. leaves were obtained in June 2024 from Abeli, Kendari city, Southeast Sulawesi, Indonesia (3°59'14.2" S, 122°36'14.8" E). For simplicity, from now on the authors abbreviated the name *A. marina* (Forssk.) Vierh as AM. This plant was identified by the Laboratory of Biology Education, Universitas Halu Oleo, Indonesia, under registration number 15/BIO/PB/VI/2024. Plant specimens were stored in the Herbarium with code HERB-FKIP-UHO-AM-2024, and AM leaves were wet-sorted to remove impurities, washed, thinly sliced, and air-dried. The crude simplicity of AM leaves (728 g) was macerated with methanol as the solvent and evaporated into a crude extract (83 g) with a yield of 11.40% (w/w).

LC-HRMS was used as a powerful tool for qualitative analysis to characterize the chemical components of AM (16). The chromatographic separation was performed using a Thermo Scientific™ Vanquish™ UHPLC Binary Pump coupled with Orbitrap high-resolution mass spectrometry (Thermo Scientific™ Q Exactive™ Hybrid Quadrupole-Orbitrap™ High-Resolution Mass Spectrometer) to reveal metabolic profile of AM extract. The analysis was done using an analytical column of Thermo Scientific™ Accucore™ Phenyl-Hexyl 100 mm  $\times$  2.1 mm ID  $\times$  2.6  $\mu$ m. The details of LC-HRMS measurement were previously described (17).

Prediction of drug-likeness properties for each compound was performed using SwissADME web server (<http://www.swissadme.ch/>) (18). Drug-likeness properties were predicted based on the Lipinsky rule of 5, which included molecular weight  $\leq$ 500 Da, the number of hydrogen bond donors  $\leq$ 5, the number of hydrogen bond acceptors  $\leq$ 10, and the log *P* value  $\leq$ 5. Compounds violating the Lipinsky rule of 5 more than one criterion

were excluded from further study. The SMILE codes for each compound were inserted into the webserver to obtain drug-likeness properties.

#### Gene identification associated with HCV

Target prediction due to compounds of AM was performed using SwissTargetPrediction (SwissTargetPrediction) and SEA (<https://sea.bkslab.org>) database using the input SMILE code of each compound (19,20).

The genes associated with HCV were predicted using OMIM (<https://www.omim.org>) and GeneCard (<https://www.genecards.org>) (21,22). These genes were filtered based on the top 500 targets (23); the results of the disease targets and compounds were then filtered and combined into a Venn diagram using Bioinformatics and System Biology (<https://bioinformatics.psb.ugent.be/webtools/Venn>).

#### Protein-protein interaction (PPI) network and core target selection

PPI was built using the String Database (<https://string-db.org>) in which the protein target was limited to the species "*Homo sapiens*" and high confidence 0.007 with the other parameters set to default. Subsequently, PPI network was imported into Cytoscape v3.10.2 (24) for subsequent analysis.

#### Gene ontology (GO) analysis and KEGG path

The Metascape (<https://www.metascape.org>) and shinyGO 0.80 databases were used to perform GO analysis to evaluate biological functions, cellular processes, and molecular components of predicted protein targets (25-27). KEGG pathway analysis revealed metabolic pathways or molecular signals affected by the compounds and target compounds of AM and HCV. The obtained paths were then considered as the working paths of the compounds.

#### Molecular docking

Molecular docking was performed on the 3 best targets using the 3D protein structures of interleukin 6 (IL-6), signal transducer and activator of transcription 3 (STAT3), and tumor necrosis factor  $\alpha$  (TNF $\alpha$ ), which were obtained by querying the PDB database (<https://www.rcsb.org>). The 2D structures of AM compounds identified from LC-HRMS analysis were converted to 3D structures using the Maestro LigPrep Module and OPLS-2005 forcefield (28,29). Protein and ligand preparations were prepared according to the previous protocol (28) using Maestro Schrödinger 11.1.012 release 2017-1 software (Schrödinger, New York, NY, USA) (29). Prednisolone, a corticosteroid prescribed for the treatment of a wide range of inflammatory diseases was used as a positive control when docking to IL-6 (30). The C $\gamma$  atom of the Phenylalanine-103 of IL-6 with x, y, and z coordinate values of 16.471, 48.983, and 82.154, respectively, was

assigned as the centroid, and the binding site radius was set to 12 Å (30). Meanwhile, native ligands KQF and 307 were employed as reference compounds for docking to STAT3 and TNF (31), respectively.

#### Molecular dynamics simulation

The receptor-ligand complexes were prepared and utilized to develop MD simulation systems. These complexes were immersed in an orthorhombic water box with a 10 Å buffer, employing the predefined SPC water model (32). A total of 0.15 M NaCl concentration was incorporated to neutralize the systems. OPLS3 force field was applied to build the systems using Desmond System Builder in Maestro on a Linux platform (33). This module was then used to configure the relaxation, minimization, and production runs following established protocol (28).

Desmond Simulation Interaction Diagram (SID) tool in Maestro was used to analyze the simulation trajectory by calculating root-mean-square deviation (RMSD), root-mean-square fluctuation (RMSF), and residue-ligand interactions and contacts. RMSD plots for protein C $\alpha$ , obtained from SID analysis were assessed to confirm the convergence of each MD simulation. A stable and relatively flat plot signified that the system had attained a steady state.

#### Cells culture and virus preparation

The cells in this study came from cloned human liver cancer cell lines (Huh7it-1) (34,35). They were grown in DMEM, which had extra amino acids (Gibco-Invitrogen), 10% fetal bovine serum (Biowest), and kanamycin (Sigma-Aldrich). The cells were kept in an incubator with 5% CO $_2$  at 37 °C. The virus used was the JFH-1 strain of HCV genotype 2a (36).

#### Antiviral activity

The antiviral tests were done following the method from Apriyanto et al (36). Cells got infected with the virus at a multiplication of infection of 0.1 and were given AM leaf extract in amounts of 0.01, 0.1, 1, 10, 50, and 100  $\mu$ g/mL. After staying at 37 °C for 2 hours, the virus was washed away, and the cells stayed with the extract for 46 more hours at the same temperature. The liquid from the culture was taken to check virus levels, following Apriyanto and colleagues' method (36). The IC $_{50}$  value was figured out using SPSS probit analysis (35).

## Results

#### LC-HRMS and drug-likeness analysis

LC-HRMS analysis was used to identify the compounds present in AM extract. Through analysis of the data, including molecular formulas, fragment ions, and chemical structure information sourced from literature and public databases, 74 compounds were identified (Table S1).

The authors analyzed drug-likeness properties of the 74 compounds, and the results were displayed in Table S2, which employed the Lipinsky rule criteria for screening and determined that the compound that violated more than one Lipinsky rule of 5, because of this, was excluded from the next study. In addition, the authors found out that 4 compounds (assigned as red color in Table S1) violated more than one Lipinsky rule of 5, such as Comp37, Comp51, Comp59, and Comp64. Therefore, only 70 compounds were selected for the subsequent network pharmacology studies.

### The target genes of *Avicennia marina* compounds and HCV

Collection of 1534 targets for AM compounds was obtained through SwissTargetPrediction and SEA databases, whereas 694 gene targets for HCV were obtained through the OMIM and GeneCard databases. Common targets related to HCV and their corresponding targets were obtained using a Venn diagram, and 88 potential HCV genes were selected and considered common targets (Figure 1).

PPI was built using the Search Tool for the Retrieval of Interacting Genes/Proteins (STRING) (<http://string-db.org>). The resulting network was analyzed using Cytoscape

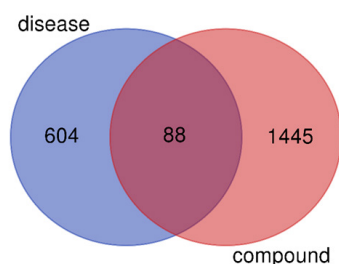


**Figure 1.** Venn diagram of the common target of hepatitis C virus-*Avicennia marina*. Blue indicates the genes of hepatitis C virus, orange the targets of compounds of *A. marina*, and red common targets.

v3.10.2 (<https://cytoscape.org>), and the protein with the highest number of interactions with other proteins was identified (Figure 2).

The CytoHubba plug-in was used to identify core targets based on their degree, closeness, and betweenness values (Table 1), which were consistently shown to be IL-6, STAT3, TNF, SRC, EGFR, AKT1, CTNNB1, PI3KCA, TLR4, and BCL2 (Figure S1).

The analysis considers several criteria, such as degree, betweenness centrality, and closeness centrality, in which IL-6 consistently showed higher values than the other proteins. The degree indicated the number of direct interactions of a node, where a higher number of direct connections indicated a more significant role it played in the network. Betweenness centrality assessed the shortest path of all node pairs, which stresses certain nodes that facilitated communication in the network. Closeness centrality was defined as the opposite of the shortest path average between nodes in the network, where a higher value indicated a higher centrality level and faster signal transmission to other nodes in the network (37).

### KEGG and GO analysis

The shiny GO 0.80 platform was used to perform functional analysis of KEGG and GO based on 3 categories namely biological process, cellular components, and molecular function. As many as overlapping 88 targets between AM and HCV were obtained, with false discovery rate (FDR)/ $P < 0.05$ , which indicated that it was statistically significant (38). Figure 3 displayed the top 10 enrichment of each category listed based on  $P$  value, and GO biological process enrichment showed the protein phosphorylation with the highest  $P$  value (Figure 3a). The cellular component indicating receptor complex had the highest  $P$  value (Figure 3b), the transmembrane receptor protein kinase activity as a molecular function had the highest  $P$  value (Figure 3c), and KEGG pathway with

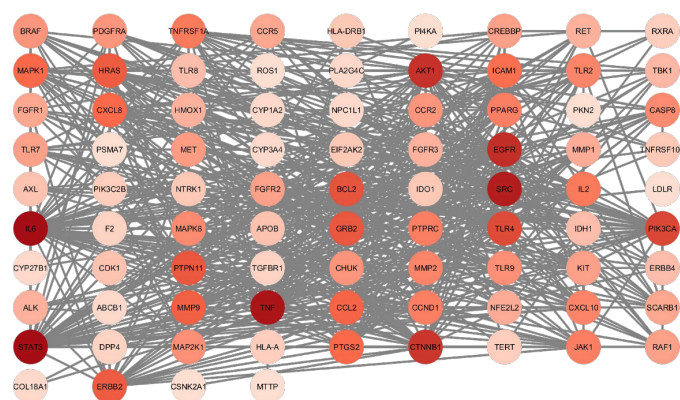


**Figure 2.** The network diagram of protein-protein interaction (PPI) of *Avicennia marina* against hepatitis C virus. The more intense the color, the higher the degree of the genes. PPI interaction highlighted interleukin-6 (IL-6), signal transducer and activator of transcription 3 (STAT3), and tumor necrosis factor- $\alpha$  (TNF- $\alpha$ ) as key proteins associated with hepatitis C virus pathways.



**Table 1.** Top 10 proteins with their degree, closeness centrality, and betweenness centrality values

| Name  | Degree | Closeness centrality | Betweenness centrality |
|---|--------|----------------------|------------------------|
| Interleukin-6 (IL-6)  | 44     | 0.661                | 0.142                  |
| Signal transducer and activator of transcription 3 (STAT3)                      | 44     | 0.651                | 0.120                  |
| Tumor necrosis factor- $\alpha$ (TNF- $\alpha$ )                                | 42     | 0.636                | 0.095                  |
| Sarcoma (SRC)   | 40     | 0.632                | 0.077                  |
| Epidermal growth factor receptor (EGFR)   | 36     | 0.609                | 0.067                  |
| AKT serine/threonine kinase 1 (AKT1)  | 35     | 0.604                | 0.058                  |
| Catenin beta 1 (CTNNB1)   | 34     | 0.596                | 0.083                  |
| Phosphatidylinositol-4,5-bisphosphate 3-kinase catalytic subunit alpha (PI3KCA) | 30     | 0.553                | 0.054                  |
| Toll-like receptor 4 (TLR4)   | 29     | 0.571                | 0.022                  |
| B-cell lymphoma 2 (BCL2)  | 27     | 0.564                | 0.020                  |

Degree: The number of direct interactions of a node; Closeness centrality: Opposite of the shortest path average between nodes in the network; Betweenness centrality: The shortest path of all node pairs (37).

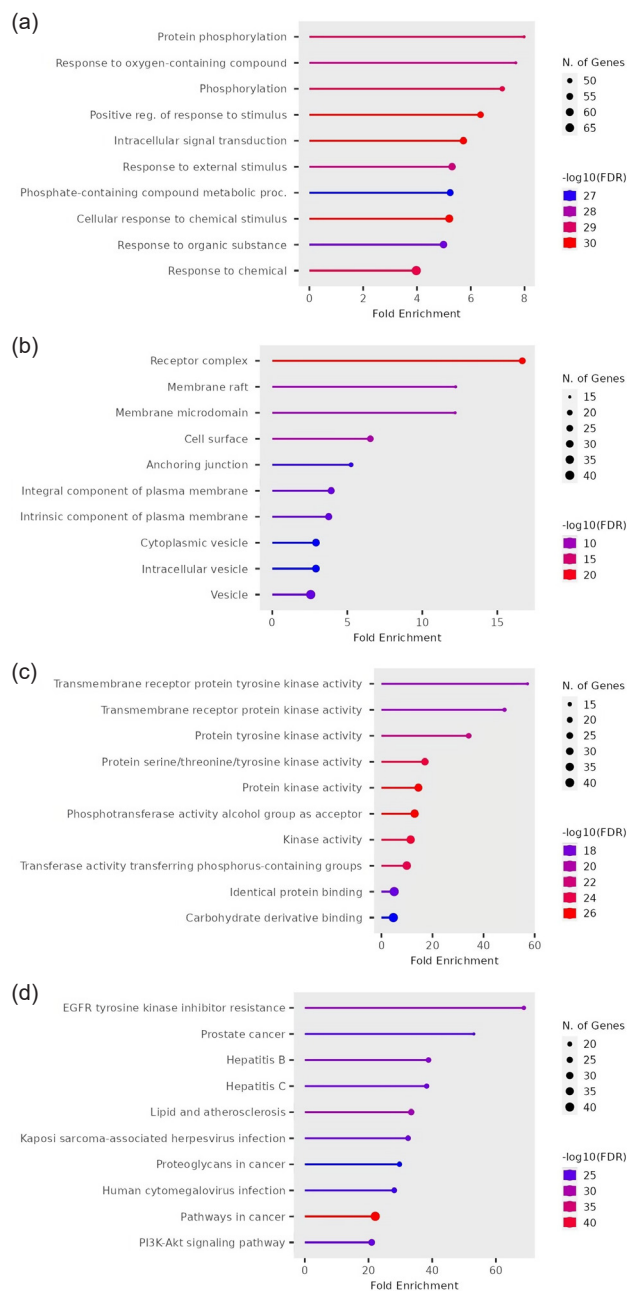


**Figure 3.** The diagram of enrichment analysis of gene ontology (GO) for *Avicennia marina* compounds with false discovery rate (FDR) < 0.7. (a) biological process (b) cellular component, (c) molecular function, (d) Kyoto Encyclopedia of Genes and Genomes (KEGG) pathway of *A. marina* compounds.

the highest *P* value was EGFR tyrosine kinase inhibitor resistance (Figure 3d), in which this pathway correlated with HCV. Protein phosphorylation, receptor complexes, transmembrane receptor protein tyrosine kinase activity, and EGFR tyrosine kinase inhibitor resistance were associated with HCV treatment in terms of biological processes, cellular components, molecular functions, and KEGG pathways, respectively.

KEGG enrichment analysis showed overlapping targets between *A. marina* and HCV, particularly those related to the signal path of HCV (Figure 4). By integrating PPI network PPI, enrichment analysis of KEGG signal path identified IL-6, STAT3, and TNF involved in a variety of signaling pathways, including HCV signal pathway. Based on this analysis, the genes with crucial roles identified were IL-6, STAT3, and TNF as target candidates.

**Molecular docking**

Based on the network pharmacology study, 3 compounds were identified to target IL-6, 6 compounds targeted STAT3, and 3 compounds targeted TNF- $\alpha$ . Furthermore, the authors performed molecular docking analysis of these compounds for each target. Structures of the Prednisolone, Comp28, Comp63 and their docking conformations with IL-6 are depicted in Figure 5, while the structures of Comp22 and its docking conformation to IL-6 are depicted in Figure S2.

Comp63 produced more Hbond interactions with Lys105, Glu114, Ile194, Gln196, and Glu286, as compared to the positive control Prednisolone with Hbond with Cys102, Gln190, and Glu283. The binding energy of Comp63 (-7.346 kcal/mol) was also lower than Prednisolone (-3.940 kcal/mol). Comp28 (-3.490 kcal/mol) and Comp22 (-1.665 kcal/mol) showed fewer Hbond interactions with residues Gln196, Glu286, and Lys105 in the case of Comp22.

In the meantime, as many as 6 compounds were identified to target STAT3, that was Comp15, Comp23, Comp25, Comp28, Comp58, and Comp72. The structures of these compounds and their docking conformations with STAT3 were shown in Figure S3. The binding energy of the native ligand of STAT3 (KQV) was -10.616 kcal/mol, while those of Comp15, Comp23, Comp25, Comp28, Comp58, and Comp72 were -4.192 kcal/mol, -4.385 kcal/mol, -2.546 kcal/mol, -4.182 kcal/mol, -1.692 kcal/mol, and -2.893 kcal/mol, respectively, which were higher than the native ligand.

The authors also performed molecular docking with TNF- $\alpha$  as the third-best target. A total of 3 compounds were identified as targets of TNF- $\alpha$ : Comp4, Comp7, and Comp48. For comparison, native ligand 307 was used as a reference (31). The binding energy of the native ligand of TNF- $\alpha$  (307) was -6.102 kcal/mol, while those of Comp4, Comp7, and Comp48 were -6.405 kcal/mol, -4.097 kcal/mol,

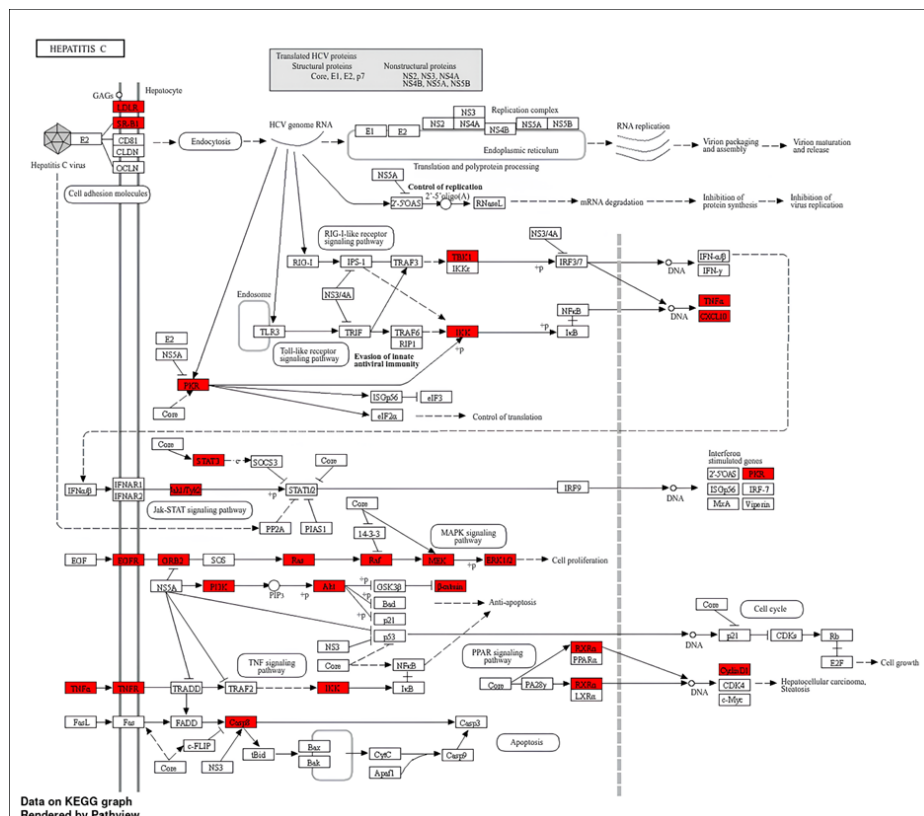


**Figure 4.** Kyoto Encyclopedia of Genes and Genomes (KEGG) pathway of hepatitis C virus. The red colors indicate the genes in common targets.

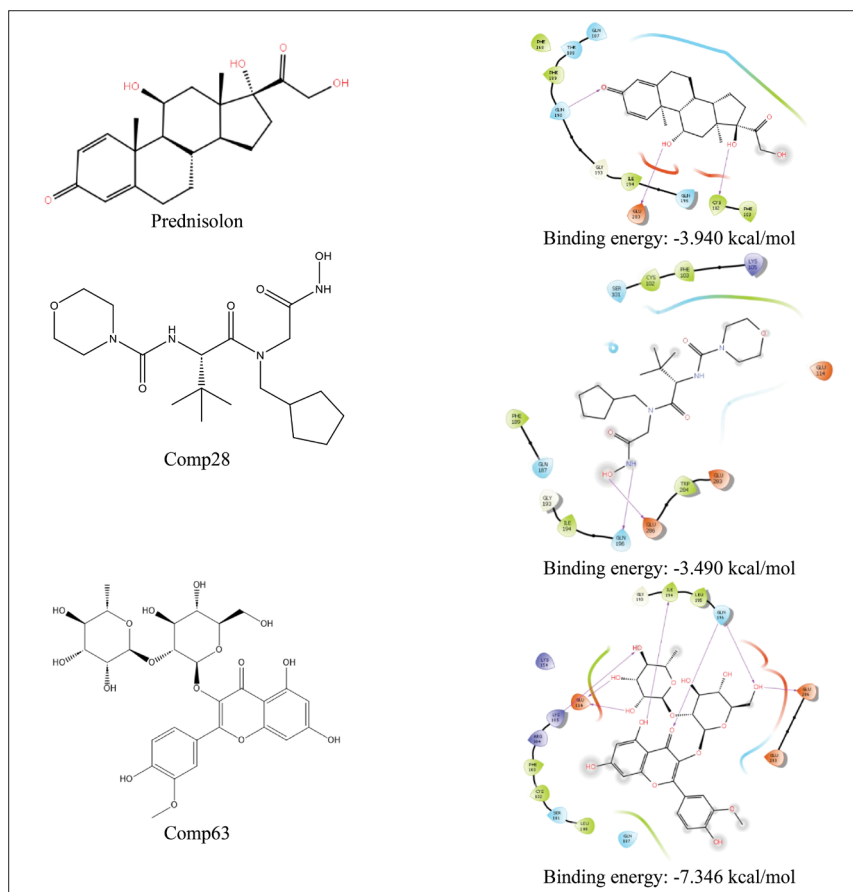


**Figure 5.** Structures of the prednisolone, Comp28, Comp63 and their docking conformations with interleukin-6 (IL-6).

mol, and -4.798 kcal/mol, respectively. The structures of these compounds and their docking conformations with TNF- $\alpha$  were shown in Figure S4.

#### Molecular dynamics simulation

RMSD plot of protein C $\alpha$  of Prednisolone and Comp63 bound to IL-6 is depicted in Figure 6, while those of KQV and Comp23 bound to STAT3 are depicted in Figure S5. This showed that the protein C $\alpha$  was relatively more stable in Prednisolone compared to Comp63 system. Prednisolone system tended to be stable after ~50 ns, while Comp63 was stable after ~110 ns. Furthermore, the protein C $\alpha$  of KQV and Comp23 systems were both stable after ~75 ns. The flexibility of each compound was assessed using RMSF,

which reflected local conformational changes along the protein backbone during the simulation. RMSF patterns for Prednisolone and Comp63 systems (Figure 6) were similar, as were for KQV and Comp23 systems (Figure S5), suggesting that ligand binding did not cause significant alterations in the protein structures. Residues with higher fluctuations were primarily located in the loop regions for both the 1N26 and 6NJS systems.

#### Protein-ligand interaction analysis

SID was examined to analyze protein-ligand interactions during molecular dynamics simulation (MDS). Interactions with residues that persisted for more than 20% of the simulation time for Prednisolone and Comp63

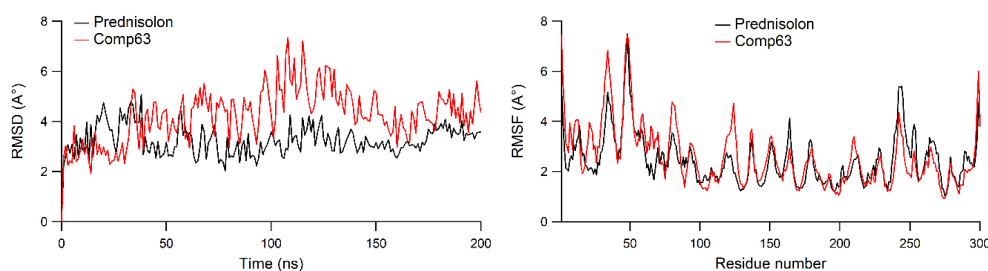


**Figure 6.** Root-mean-square deviation (RMSD) (left) and root-mean-square fluctuation (RMSF) (right) plots of protein C $\alpha$  in Prednisolone and Comp63 systems.

bounds to IL-6 are illustrated in Figure 7, while those for KQV and Comp23 bounds to STAT3 are depicted in Figure S6. In Prednisolone system (Figure 7a), hydrogen bond (Hbond) interactions were identified between the ligand and Leu100 (30% occupancy) as well as Thr188 (37% occupancy). In Comp63 system (Figure 7b), Hbond was observed between the ligand and Gln196 (42% occupancy), Lys185 (41% occupancy), and Arg210 (34% occupancy), suggesting the role in stabilizing the binding of Comp63.

In the 6NJS system (Figure S6), Hbond interactions were observed between KQV with residues Glu612

(occupancy 97%), Ser611 (occupancy 100%), Ser613 (occupancy 100%), Ser636 (occupancy 80%), Glu638 (occupancy 99%). In addition, water-mediated Hbond was also observed with Glu638. While in the Comp23 system, Ser611 (occupancy 47%), Glu612 (occupancy 46%), and Ser613 (occupancy 41%) participated in Hbond interactions. In addition, it was clear that Comp23 binding had diminished effects on ligand protein.

*In vitro* anti-HCV study

*In vitro* anti-HCV study of AM leaves extract was conducted to evaluate its antiviral effects against HCV at

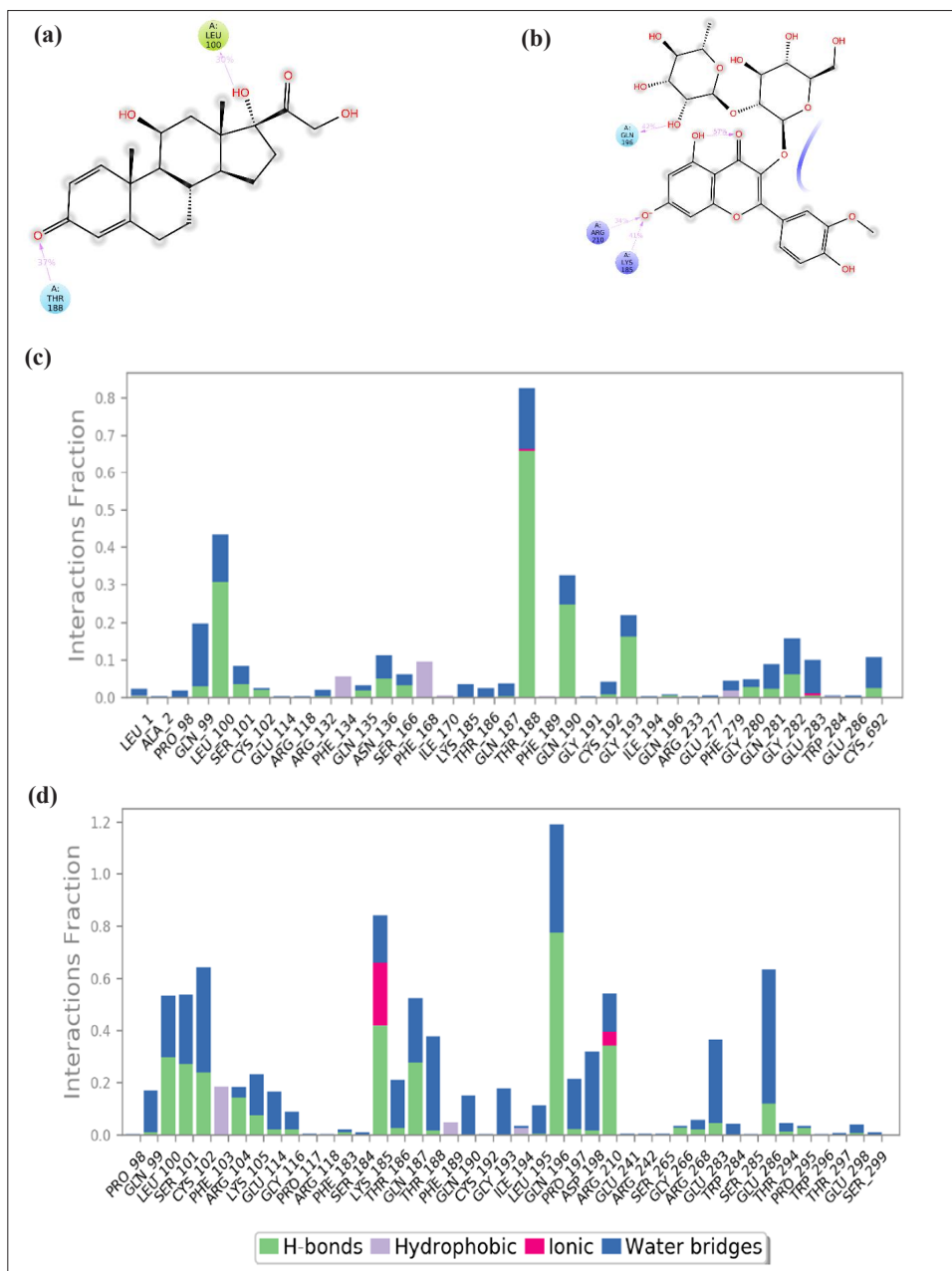


**Figure 7.** The two-dimensional ligand protein interaction diagram recorded during MD simulations for Prednisolone (a) and Comp63 (b) systems. (c) and (d) indicate protein-ligand contacts during MD simulations for Prednisolone and Comp63 (d) systems, respectively. Interaction fraction greater than 1 is because of multiple contacts on one residue.



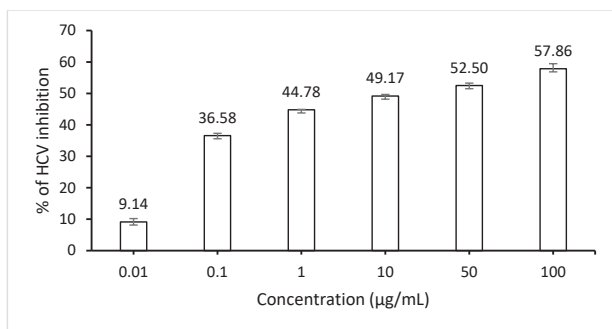


**Figure 8.** Inhibition of hepatitis C virus infection of *Avicennia marina* (0.01 to 100 µg/mL) determined by virus titers in the cell culture. Data are presented as means  $\pm$  standard deviation of data from triplicate.

various concentrations. As shown in Figure 8, AM leaves extract effectively inhibited HCV infection, with  $IC_{50}$  value of  $12.664 \pm 0.984$  µg/mL.

## Discussion

The leaves extract of AM was investigated for its potential to inhibit HCV infection. The network pharmacology analysis revealed IL-6, STAT3, TNF, SRC, EGFR, AKT1, CTNBN1, PIK3CA, TLR4, and BCL2 as core targets. Molecular docking performed on the top 3 protein targets, namely IL-6, STAT3, and TNF. IL-6 was a multifunctional cytokine that influenced a wide range of biological processes via various mechanisms. Alterations in cytokine activity were observed in HCV infections, with an imbalance between pro-inflammatory and anti-inflammatory cytokine production, which played a critical role in immunopathogenesis. Elevated IL-6 levels were linked to increased disease severity and activity in numerous chronic conditions, including chronic hepatitis, liver cirrhosis, and hepatocellular carcinoma (39). Therefore, inhibition of IL-6 contributed to the slowdown of HCV progression. In this study, 2 compounds, Comp28 and Comp63, had comparable and lower binding energies in comparison with Prednisolone, which indicated their potential to inhibit IL-6.

The signal transducer and activator of transcription 3 (STAT3) was a cytoplasmic signal transduction factor in the Janus kinase (JAK) pathway that played a crucial role in mediating liver damage. JAK-STAT pathway served as a key signaling mechanism in mammals, transmitting signals from cytokine receptors and involved numerous cytokines and growth factors. STAT3 was particularly significant in the pathophysiology of liver disorders and played a critical role in liver cancer. Therefore, STAT3 activation promoted the growth, metastasis, and survival of hepatocellular carcinoma (40). In this study, the 6 compounds docked to STAT3 had higher binding energies than the reference compounds (Figure S3).

Numerous studies have suggested that the Persistence

and activity of HCV infection are linked to its interaction with the TNF- $\alpha$ . TNF- $\alpha$  influenced disease outcomes by inducing the death of infected cells. In addition, the pathophysiology of hepatitis C involved viral infection that elevated pro-inflammatory markers, such as TNF- $\alpha$  and IL-6, which exerted systemic effects (40). Additionally, elevated TNF- $\alpha$  levels were observed in HCC patients with hepatocellular carcinoma. TNF- $\alpha$  concentrations in the sera of HBV and HCV patients were significantly higher than those in the control group, with statistically significant differences between both groups ( $P < 0.05$ ) (39). In chronic hepatitis C, TNF- $\alpha$  contributed to the disease pathogenesis by inducing hepatocyte apoptosis and sustaining liver inflammation (41). Patients with HCV infection exhibited elevated levels of circulating TNF- $\alpha$  (42). Serum TNF- $\alpha$  levels in HCV patients were higher and showed a positive correlation with the severity of liver disease. In this current study, the authors identified Comp4, which had an affinity comparable to the reference compound, and Comp7 and Comp48, which had slightly higher affinities, as potential inhibitors of TNF- $\alpha$ .

Several studies have reported the antiviral activities of AM extracts. For instance, Behbahani et al showed the antiherpetic substances of the crude methanol leaves extract of AM with an  $EC_{50}$  of 10 µg/mL (43). Beula et al reported leaves extract of AM to inhibit reverse transcriptase enzyme with  $IC_{50}$  of 403.91 µg/mL (44). AM leaves were also reported by Kathiresan et al and Premanathan et al to have antiviral activity against the hepatitis B virus Newcastle disease virus (45,46). Premanathan et al also reported that AM inhibited encephalomyocarditis virus at  $EC_{50}$  46.7 µg/mL (47). Briefly, the  $IC_{50}$  value of AM leaves extract, shown in this study, was comparable with the previous studies.

The good anti-HCV activity of AM methanolic extract was in good accordance with a good affinity of Comp63 to IL-6, which was isorhamnetin-3-O-neohesperidoside, a member of flavonoids. Isorhamnetin was previously shown to have strong antiviral potency against the influenza virus (48). In the MDS, the average RMSD and RMSF values of Comp63 systems were higher than Prednisolone system, and Comp63 was stabilized during the 200-ns simulation. In addition, Comp4, which was an alkaloid iminosugar derivative with a good affinity to TNF- $\alpha$ , was -6.102 kcal/mol. Previous studies have shown that iminosugar derivatives are potent against HCV (49,50). The authors acknowledged the limitations of this current study, as the data presented were needed to validate through a large number of experimental studies both *in vitro* and *in vivo* assays, which could be the next project.

## Conclusions

This study demonstrated the potential of AM methanolic leaves extract to inhibit HCV infection through a combination of network pharmacology, molecular

docking, and *in vitro* validation. Key compounds, such as Comp63 and Comp4, showed strong binding affinities to IL-6 and TNF- $\alpha$ , respectively, outperforming native ligands. The extract exhibited significant anti-HCV activity with an IC<sub>50</sub> value of 12.664 $\pm$ 0.984  $\mu$ g/mL, highlighting its therapeutic potential. These findings provide a foundation for further research and development of AM as a natural remedy for HCV.

### Acknowledgment

The authors are grateful to Arfan, MS, who provided assistance in the early stage of the study.

### Authors' contribution

**Conceptualization:** Muhammad Arba.

**Data curation:** Fathar Muhamad Irfansya Hatma, Sunandar Ihsan.

**Formal analysis:** Sunandar Ihsan.

**Funding acquisition:** Muhammad Arba.

**Investigation:** All authors.

**Methodology:** All authors.

**Project administration:** Fathar Muhamad Irfansya Hatma.

**Resources:** Setyanto Tri Wahyudi, Tutik Sri Wahyuni, Muhammad Arba.

**Software:** Setyanto Tri Wahyudi, Muhammad Arba.

**Supervision:** Muhammad Arba.

**Validation:** All authors.

**Visualization:** All authors.

**Writing—original draft:** Fathar Muhamad Irfansya Hatma, Sunandar Ihsan.

**Writing—review & editing:** Muhammad Arba.

### Conflict of interests

None to declare.

### Ethical considerations

Not applicable.

### Funding/Support

Hibah Penelitian Fundamental Kemenristek-Dikti Republic of Indonesia through contract number: 20/UN29.20/PG/2024.

### Supplementary files

Supplementary file 1 contains Tables S1-S2 and Figures S1-S6.

### References

- Mohd Hanafiah K, Groeger J, Flaxman AD, Wiersma ST. Global epidemiology of hepatitis C virus infection: new estimates of age-specific antibody to HCV seroprevalence. *Hepatology*. 2013;57(4):1333-42. doi: 10.1002/hep.26141.
- Lasmanovich R, Shaked O, Sivan A, Barak I, Nahari M, Mor O, et al. Hepatitis C virus prevalence, medical status awareness and treatment engagement among homeless people who use drugs: results of a street outreach study. *Subst Abuse*. 2022;16:11782218221095871. doi: 10.1177/11782218221095871.
- Yang C, Lv F, Yang J, Ding D, Cui L, Han Y. Surveillance and management of hepatocellular carcinoma after treatment of hepatitis C with direct-acting antiviral drugs. *Ann Hepatol*. 2024;30(2):101582. doi: 10.1016/j.aohep.2024.101582.
- Lam AM, Murakami E, Espiritu C, Steuer HM, Niu C, Keilman M, et al. PSI-7851, a pronucleotide of beta-D-2'-deoxy-2'-fluoro-2'-C-methyluridine monophosphate, is a potent and pan-genotype inhibitor of hepatitis C virus replication. *Antimicrob Agents Chemother*. 2010;54(8):3187-96. doi: 10.1128/aac.00399-10.
- Bhattacharjee C, Singh M, Das D, Chaudhuri S, Mukhopadhyay A. Current therapeutics against HCV. *Virusdisease*. 2021;32(2):228-43. doi: 10.1007/s13337-021-00697-0.
- Hayes CN, Chayama K. Why highly effective drugs are not enough: the need for an affordable solution to eliminating HCV. *Expert Rev Clin Pharmacol*. 2017;10(6):583-94. doi: 10.1080/17512433.2017.1313111.
- Wahyuni TS, Utsubo CA, Hotta H. Promising anti-hepatitis C virus compounds from natural resources. *Nat Prod Commun*. 2016;11(8):1193-200.
- Parthiban A, Sivasankar R, Sachithanandam V, Khan SA, Jayshree A, Murugan K, et al. An integrative review on bioactive compounds from Indian mangroves for future drug discovery. *S Afr J Bot*. 2022;149:899-915. doi: 10.1016/j.sajb.2021.10.004.
- Wu Z, Shang X, Liu G, Xie Y. Comparative analysis of flavonoids, polyphenols and volatiles in roots, stems and leaves of five mangroves. *PeerJ*. 2023;11:e15529. doi: 10.7717/peerj.15529.
- Mitra S, Naskar N, Lahiri S, Chaudhuri P. A study on phytochemical profiling of *Avicennia marina* mangrove leaves collected from Indian Sundarbans. *Sustain Chem Environ*. 2023;4:100041. doi: 10.1016/j.scenv.2023.100041.
- Zandi K, Taherzadeh M, Tajbakhsh S, Yaghoubi R, Rastian Z, Sartavi K. Antiviral activity of *Avicennia marina* leaf extract on HSV-1 and vaccine strain of polio virus in vero cells. *Int J Infect Dis*. 2008;12:e298. doi: 10.1016/j.ijid.2008.05.800.
- Lin CK, Tseng CK, Chen KH, Wu SH, Liaw CC, Lee JC. Betulinic acid exerts anti-hepatitis C virus activity via the suppression of NF- $\kappa$ B- and MAPK-ERK1/2-mediated COX-2 expression. *Br J Pharmacol*. 2015;172(18):4481-92. doi: 10.1111/bph.13233.
- Sheela Devi A, Rajkumar J, Beenish TK. Detection of antibacterial compound of *Avicennia marina* against pathogens isolated from urinary tract infected patients. *Asian J Chem*. 2014;26(2):458-60. doi: 10.14233/ajchem.2014.15442.
- Alshehri FF, Alshehri ZS. Network pharmacology-based screening of active constituents of *Avicennia marina* and their clinical biochemistry related mechanism against breast cancer. *J Biomol Struct Dyn*. 2024;42(9):4506-21. doi: 10.1080/07391102.2023.2220801.
- Murdiana HE, Murwanti R, Fakhruddin N, Ikawati Z. Multi-target mechanism of polyherbal extract to treat diabetic

- foot ulcer based on network pharmacology and molecular docking. *J Herbm Pharm*. 2024;13(2):289-99. doi: 10.34172/jhp.2024.49362.
16. Zubair MS, Maulana S, Widodo A, Pitopang R, Arba M, Hariono M. GC-MS, LC-MS/MS, docking and molecular dynamics approaches to identify potential SARS-CoV-2 3-chymotrypsin-like protease inhibitors from *Zingiber officinale* Roscoe. *Molecules*. 2021;26(17):5230. doi: 10.3390/molecules26175230.
  17. Windarsih A, Suratno, Warmiko HD, Indrianingsih AW, Rohman A, Ulumuddin YI. Untargeted metabolomics and proteomics approach using liquid chromatography-Orbitrap high resolution mass spectrometry to detect pork adulteration in *Pangasius hypophthalmus* meat. *Food Chem*. 2022;386:132856. doi: 10.1016/j.foodchem.2022.132856.
  18. Daina A, Michielin O, Zoete V. SwissADME: a free web tool to evaluate pharmacokinetics, drug-likeness and medicinal chemistry friendliness of small molecules. *Sci Rep*. 2017;7:42717. doi: 10.1038/srep42717.
  19. Daina A, Michielin O, Zoete V. SwissTargetPrediction: updated data and new features for efficient prediction of protein targets of small molecules. *Nucleic Acids Res*. 2019;47(W1):W357-64. doi: 10.1093/nar/gkz382.
  20. Keiser MJ, Roth BL, Armbruster BN, Ernsb5erger P, Irwin JJ, Shoichet BK. Relating protein pharmacology by ligand chemistry. *Nat Biotechnol*. 2007;25(2):197-206. doi: 10.1038/nbt1284.
  21. Rebhan M, Chalifa-Caspi V, Prilusky J, Lancet D. GeneCards: a novel functional genomics compendium with automated data mining and query reformulation support. *Bioinformatics*. 1998;14(8):656-64. doi: 10.1093/bioinformatics/14.8.656.
  22. Amberger JS, Bocchini CA, Schiettecatte F, Scott AF, Hamosh A. OMIM.org: Online Mendelian Inheritance in Man (OMIM®), an online catalog of human genes and genetic disorders. *Nucleic Acids Res*. 2015;43(D1):D789-98. doi: 10.1093/nar/gku1205.
  23. Jiang LR, Qin Y, Nong JL, An H. Network pharmacology analysis of pharmacological mechanisms underlying the anti-type 2 diabetes mellitus effect of guava leaf. *Arab J Chem*. 2021;14(6):103143. doi: 10.1016/j.arabjc.2021.103143.
  24. Shannon P, Markiel A, Ozier O, Baliga NS, Wang JT, Ramage D, et al. Cytoscape: a software environment for integrated models of biomolecular interaction networks. *Genome Res*. 2003;13(11):2498-504. doi: 10.1101/gr.1239303.
  25. Kanehisa M, Furumichi M, Tanabe M, Sato Y, Morishima K. KEGG: new perspectives on genomes, pathways, diseases and drugs. *Nucleic Acids Res*. 2017;45(D1):D353-61. doi: 10.1093/nar/gkw1092.
  26. Zhou Y, Zhou B, Pache L, Chang M, Khodabakhshi AH, Tanaseichuk O, et al. Metascape provides a biologist-oriented resource for the analysis of systems-level datasets. *Nat Commun*. 2019;10(1):1523. doi: 10.1038/s41467-019-09234-6.
  27. Ge SX, Jung D, Yao R. ShinyGO: a graphical gene-set enrichment tool for animals and plants. *Bioinformatics*. 2020;36(8):2628-9. doi: 10.1093/bioinformatics/btz931.
  28. Arba M, Wahyudi ST, Brunt DJ, Paradis N, Wu C. Mechanistic insight on the remdesivir binding to RNA-dependent RNA polymerase (RdRp) of SARS-cov-2. *Comput Biol Med*. 2021;129:104156. doi: 10.1016/j.compbio.2020.104156.
  29. Sastry GM, Adzhigirey M, Day T, Annabhimoju R, Sherman W. Protein and ligand preparation: parameters, protocols, and influence on virtual screening enrichments. *J Comput Aided Mol Des*. 2013;27(3):221-34. doi: 10.1007/s10822-013-9644-8.
  30. Santhosh Kumar S, Sajeli Begum A, Hira K, Niazi S, Prashantha Kumar BR, Araya H, et al. Structure-based design and synthesis of new 4-methylcoumarin-based lignans as pro-inflammatory cytokines (TNF- $\alpha$ , IL-6 and IL-1 $\beta$ ) inhibitors. *Bioorg Chem*. 2019;89:102991. doi: 10.1016/j.bioorg.2019.102991.
  31. He MM, Smith AS, Oslob JD, Flanagan WM, Braisted AC, Whitty A, et al. Small-molecule inhibition of TNF- $\alpha$ . *Science*. 2005;310(5750):1022-5. doi: 10.1126/science.1116304.
  32. Mark P, Nilsson L. Structure and dynamics of the TIP3P, SPC, and SPC/E water models at 298 K. *J Phys Chem A*. 2001;105(43):9954-60. doi: 10.1021/jp003020w.
  33. Harder E, Damm W, Maple J, Wu C, Reboul M, Xiang JY, et al. OPLS3: a force field providing broad coverage of drug-like small molecules and proteins. *J Chem Theory Comput*. 2016;12(1):281-96. doi: 10.1021/acs.jctc.5b00864.
  34. Wahyuni TS, Permatasari AA, Widiandani T, Fuad A, Widyawaruyanti A, Aoki-Utsubo C, et al. Antiviral activities of *Curcuma* genus against hepatitis C virus. *Nat Prod Commun*. 2018;13(12):1579-82.
  35. Widyawaruyanti A, Tanjung M, Permanasari AA, Saputri R, Tumewu L, Adianti M, et al. Alkaloid and benzopyran compounds of *Melicope latifolia* fruit exhibit anti-hepatitis C virus activities. *BMC Complement Med Ther*. 2021;21(1):27.
  36. Apriyanto DR, Aoki C, Hartati S, Hanafi M, Kardono LBS, Arsianti A, et al. Anti-hepatitis C virus activity of a crude extract from Longan (*Dimocarpus longan* Lour.) leaves. *Jpn J Infect Dis*. 2016;69(3):213-220.
  37. Zhou W, Wang Y, Lu A, Zhang G. Systems pharmacology in small molecular drug discovery. *Int J Mol Sci*. 2016;17(2):246. doi: 10.3390/ijms17020246.
  38. Dong Q, Ren G, Li Y, Hao D. Network pharmacology analysis and experimental validation to explore the mechanism of kaempferol in the treatment of osteoporosis. *Sci Rep*. 2024;14(1):7088. doi: 10.1038/s41598-024-57796-3.
  39. Mourtzikou A, Alepaki M, Stamouli M, Pouliakis A, Skliris A, Karakitsos P. Evaluation of serum levels of IL-6, TNF- $\alpha$ , IL-10, IL-2 and IL-4 in patients with chronic hepatitis. *Inmunología*. 2014;33(2):41-50. doi: 10.1016/j.inmuno.2014.01.001.
  40. Ali FE, Abdel-Reheim MA, Hassanein EH, Abd El-Aziz MK, Althagafy HS, Badran KS. Exploring the potential of drug repurposing for liver diseases: a comprehensive study. *Life Sci*. 2024;347:122642. doi: 10.1016/j.lfs.2024.122642.
  41. Viganò M, Degasperis E, Aghemo A, Lampertico P, Colombo M. Anti-TNF drugs in patients with hepatitis B or C virus infection: safety and clinical management. *Expert Opin Biol Ther*. 2012;12(2):193-207. doi: 10.1517/14712598.2012.646986.
  42. Lee J, Tian Y, Chan ST, Kim JY, Cho C, Ou JH. TNF- $\alpha$  induced by hepatitis C virus via TLR7 and TLR8 in hepatocytes supports interferon signaling via an autocrine

- mechanism. PLoS Pathog. 2015;11(5):e1004937. doi: 10.1371/journal.ppat.1004937.
43. Behbahani M, Shanehsaz Zadeh M, Mohabatkar H. Evaluation of antiherpetic activity of crude extract and fractions of *Avicennia marina*, in vitro. Antiviral Res. 2013;97(3):376-80. doi: 10.1016/j.antiviral.2013.01.001.
  44. Beula JM, Gnanadesigan M, Rajkumar PB, Ravikumar S, Anand M. Antiviral, antioxidant and toxicological evaluation of mangrove plant from South East coast of India. Asian Pac J Trop Biomed. 2012;2(1 Suppl):S352-7. doi: 10.1016/S2221-1691(12)60187-7.
  45. Kathiresan K. Bioprospecting potential of mangrove resources. In: Patra JK, Mishra RR, Thatoi H, eds. Biotechnological Utilization of Mangrove Resources. Academic Press; 2020. p. 225-41. doi: 10.1016/b978-0-12-819532-1.00008-1.
  46. Premnathan M, Chandra K, Bajpai SK, Kathiresan K. A survey of some Indian marine plants for antiviral activity. Botanica Marina. 1992;35(4):321-4. doi: 10.1515/botm.1992.35.4.321.
  47. Premanathan M, Kathiresan K, Chandra K. Antiviral activity of marine and coastal plants from India. Int J Pharmacogn. 1994;32(4):330-6. doi:10.3109/13880209409083011.
  48. Abdal Dayem A, Choi HY, Kim YB, Cho SG. Antiviral effect of methylated flavonol isorhamnetin against influenza. PLoS One. 2015;10(3):e0121610. doi: 10.1371/journal.pone.0121610.
  49. Steinmann E, Whitfield T, Kallis S, Dwek RA, Zitzmann N, Pietschmann T, et al. Antiviral effects of amantadine and iminosugar derivatives against hepatitis C virus. Hepatology. 2007;46(2):330-8. doi: 10.1002/hep.21686.
  50. Wohlfarth C, Efferth T. Natural products as promising drug candidates for the treatment of hepatitis B and C. Acta Pharmacol Sin. 2009;30(1):25-30. doi: 10.1038/aps.2008.5.

**Copyright** © 2025 The Author(s). This is an open-access article distributed under the terms of the Creative Commons Attribution License (<http://creativecommons.org/licenses/by/4.0>), which permits unrestricted use, distribution, and reproduction in any medium, provided the original work is properly cited.